
Review of the Multiple Signal Classification and Dictionary-Adjusted Nonconvex Sparsity Encouraged Regression (MUSIC-DANSER) Algorithm for Hyperspectral Unmixing

Forrest Corcoran^{* 1}

Abstract

Hyperspectral unmixing is a family of techniques used to extract the types and corresponding abundances of materials in a remotely sensed, hyperspectral scene. These techniques are of particular interest to coastal engineers and marine biologists/ecologists because they provides important information that can be used for benthic habitat mapping (i.e. the mapping of the marine ecosystem associated with the ocean floor) in optically shallow waters. Thanks to the recent launch of the PRISMA hyperspectral spectrometer satellite by the Italian Space Agency, along with several planned hyperspectral satellite missions from NASA and ESA, hyperspectral unmixing techniques have received renewed attention in the remote sensing community. In this paper I review the Multiple Signal Classification and Dictionary-Adjusted Nonconvex Sparsity Encouraged Regression technique outlined in Fu et al., 2016.

1. Introduction

Hyperspectral imaging (HSI) is a spectrographic technology used to acquire high dimensional, multiband digital images. Each band in a hyperspectral image corresponds to a small wavelength interval, with the sum of the bands contiguously covering a large portion of the visible and infrared electromagnetic spectrum. HSI has a wide array of uses, including biomedical imaging, mineral identification for mining and petroleum prospecting, crop health monitoring in agriculture, and many more. In optically shallow coastal ocean waters, HSI is often used for benthic habitat mapping (i.e. the mapping of the marine ecosystem associated with the ocean floor), due to its ability to differentiate between various types of marine flora and identify the mineral

constituents of suspended and seafloor sediment.

Though many commercial enterprises utilize remotely sensed hyperspectral imagery, the amount of publicly available data is limited. The main source of publicly available hyperspectral imagery is NASA's Airborne Visible/Infrared Imaging Spectrometer (AVIRIS). AVIRIS is an airborne hyperspectral imaging spectrometer mounted on a high altitude aircraft to simulate satellite imagery. Because AVIRIS missions are only flown periodically and on-demand, the amount of data collected by AVIRIS pales in comparison to many spaceborne multispectral imagers. However, with the recent launch of the Italian Space Agency's PRISMA hyperspectral imager mission, along with several planned missions by NASA and ESA, interest in HSI has steadily increased among remote sensing scientists and engineers.

The techniques used to extract material level information from HSI fall into the family of techniques known as hyperspectral unmixing. While there are many different methods and approaches used to perform hyperspectral unmixing, the underlying theory is the same. In hyperspectral unmixing, the observed spectrum at each pixel is assumed to be a linear combination of the unique spectral signatures associated with the materials found in the pixel, weighted by their relative abundances. The end goal of hyperspectral unmixing is two-fold: 1) to identify the materials in the scene and 2) to determine their relative abundances in each pixel. In this paper, we review the Multiple Signal Classification and Dictionary-Adjusted Nonconvex Sparsity Encouraged Regression (MUSIC-DANSER) hyperspectral unmixing technique outlined in Fu et al., 2016 and apply it to a scene including optically shallow water.

2. Methods

Hyperspectral unmixing seeks to resolve the material constituents and their associated abundance on a pixel-by-pixel basis by assuming that the observed spectrum at each pixel is a linear combination of the spectral signatures of the constituent materials weighted by their relative sub-pixel abundance. As such, the hyperspectral linear model can be

^{*}Equal contribution ¹Department of Civil Engineering, Oregon State University. Correspondence to: Forrest Corcoran <corco-raf@oregonstate.edu>.

written as follows:

$$\mathbf{y}[l] = \sum_{n=1}^N \mathbf{a}_n s_n[l] + \mathbf{v}_n[l] \quad (1)$$

where $\mathbf{y}[l] \in \mathbb{R}^M$ is the hyperspectral measurement at pixel l , $\mathbf{a}_n \in \mathbb{R}^M$ is the spectral signature of material n , $s_n[l]$ is the relative abundance of material n in pixel l , and $\mathbf{v}_n[l] \in \mathbb{R}^M$ is noise. The number of bands associated with each pixel is denoted by M . Rewritten in matrix notation,

$$\mathbf{Y} = \mathbf{A}\mathbf{S} + \mathbf{V} \quad (2)$$

where $\mathbf{Y} = [\mathbf{y}[1], \mathbf{y}[2], \dots, \mathbf{y}[L]]^T$, $\mathbf{A} = [\mathbf{a}_1, \mathbf{a}_2, \dots, \mathbf{a}_N]^T$, $\mathbf{S} = [\mathbf{s}[1], \mathbf{s}[2], \dots, \mathbf{s}[L]]^T$, $\mathbf{s}[l] = [s_1[l], s_2[l], \dots, s_N[l]]^T$, and $\mathbf{V} = [\mathbf{v}[1], \mathbf{v}[2], \dots, \mathbf{v}[L]]^T$.

In order to determine the materials present in the scene based on their spectral signatures, it is necessary to start with a dictionary of known spectral signatures and their associated material names. We denote the dictionary $\mathbf{D} \in \mathbb{R}^{M \times K}$ where K is the number of materials in the dictionary, $\mathbf{D} = [\mathbf{d}_1, \mathbf{d}_2, \dots, \mathbf{d}_K]$ and \mathbf{d}_k is the spectral signature of the k -th material.

Rewriting the original unmixing problem using the dictionary D , we get

$$\mathbf{Y} = \mathbf{D}\mathbf{C} + \mathbf{V} \quad (3)$$

In this form, the matrix $\mathbf{C} \in \mathbb{R}^{K \times L}$ is a row sparse matrix with the k -th row of \mathbf{C} corresponding to the k -th row of \mathbf{S} and all other rows equalling $\mathbf{0}$. In order to generate \mathbf{C} , we formulate the following Collaborative Sparse Regression (CSR) optimization problem:

$$\min_{\mathbf{C} \in \mathbb{R}^{K \times L}} \|\mathbf{Y} - \mathbf{D}\mathbf{C}\|_F^2 + \lambda \|\mathbf{C}\|_{2,1} \quad (4)$$

$$s.t. \mathbf{C} \geq \mathbf{0} \quad (5)$$

where $\lambda > 0$ is a prespecified constant. The purpose of formulating the problem in this way is to seek a nonnegative, row-sparse \mathbf{C} that approximates $\mathbf{Y} = \mathbf{D}\mathbf{C} + \mathbf{V}$. The mixed norm $\|\mathbf{C}\|_{2,1} = \sum_{i=1}^K \|\mathbf{c}^i\|_2$, where \mathbf{c}^i is the i -th row of \mathbf{C} , is used to promote sparsity in the resulting abundance matrix \mathbf{C} .

Although the CSR problem formulation is convex and therefore easily solvable, we are still faced with two problems: 1) the size of the dictionary and 2) the mutual coherence of entries in the dictionary. Many spectral dictionaries, such as the USGS library used in this study, contain thousands of entries. Moreover many of these spectral entries have high

Algorithm 1 MUSIC

Input: dictionary \mathbf{D} , image Y , N

$\mathbf{U}, \mathbf{S}, \mathbf{V} = svd(\mathbf{Y})$

$U_s = U(1 : N)$

for $k = 1, \dots, K$ **do**

$$\gamma_{MUSIC}(k) = \frac{\mathbf{d}_k^T \mathbf{P}_{U_s}^\perp \mathbf{d}_k}{\|\mathbf{d}_k\|_2^2}$$

end for

determine $\hat{\Lambda} = \{\hat{k}_1, \dots, \hat{k}_{\hat{K}}\}$ such that $\gamma_{MUSIC}(\hat{k}_n) < \gamma_{MUSIC}(j)$ for any $j \notin \hat{\Lambda}$

mutual coherence with each other due to the fact that the corresponding materials are similar, such as closely related types of vegetation or different types of water. In order to resolve these issues in the CSR optimization process, we must first preprocess the dictionary using a dictionary pruning algorithm. The pruning algorithm used in this study is the Multiple Signal Classification (MUSIC) algorithm.

2.1. MUSIC

The MUSIC algorithm is a subspace method developed originally to determine the direction of arrival of incoming signals at a sensor array. In this study, we use MUSIC to prune the spectral signature dictionary by selecting the N dictionary entries that best represent the observed spectral data. In order to understand the MUSIC algorithm, it is best to consider Equation (2) without the noise variable \mathbf{V} so that we have

$$\mathbf{Y} = \mathbf{A}\mathbf{S} \quad (6)$$

Next, we let the N first left singular values of \mathbf{Y} be represented by \mathbf{U}_S . It can be shown that in this case, for some $n \in \{1, \dots, N\}$,

$$\mathbf{P}_{U_S}^\perp = \mathbf{0} \iff \mathbf{d}_k = \mathbf{a}_{k_n} \quad (7)$$

In other words, if and only if dictionary entry \mathbf{d}_k is one of the N most important spectral signatures in the scene, then \mathbf{d}_k is perpendicular to the orthogonal complement of \mathbf{U}_S . Therefore, in a noiseless case, we can use Algorithm (1) to determine the N most important spectral signatures in the scene.

Although this approach provides a good theoretical basis for determining the N most important spectral dictionary entries in an ideal case, in a realistic application the presence of noise will cause dictionary mismatches. This violates one of the key assumptions of the algorithm, that any spectral signature in the scene should match perfectly with some entry of the dictionary. Therefore, in order to apply MUSIC for the purposes of pruning the spectral dictionary, we need to modify the algorithm such that it is robust to mismatches and returns a list of the N most important adjusted dictionary entries instead.

2.2. Robust MUSIC

In order to handle mismatches between the observed spectral signatures in the scene and those found in the dictionary, we employ the Robust MUSIC (RMUSIC) algorithm. This algorithm is based on the MUSIC algorithm detailed above, but modified to satisfy the spectral mismatch model shown below:

$$\mathbf{d}_{\mathbf{k}_n} = \mathbf{a}_n + \epsilon_n \quad (8)$$

where $\epsilon_n \in \mathbb{R}^M$ and $\|\epsilon_n\| \leq \delta$ for some $\delta > 0$. This model allows us to define a new dictionary $\tilde{\mathbf{D}} = \{\mathbf{d}'_{\mathbf{k}_1}, \mathbf{d}'_{\mathbf{k}_2}, \dots, \mathbf{d}'_{\mathbf{k}_N}\}$, where $\mathbf{d}'_{\mathbf{k}_n}$ is the adjusted dictionary entry such that

$$\mathbf{d}'_{\mathbf{k}} = \mathbf{d}_{\mathbf{k}} + \mathbf{e}_{\mathbf{k}} \quad (9)$$

and $\mathbf{e}_{\mathbf{k}} \in \mathbb{R}^M$, $\|\mathbf{e}_{\mathbf{k}}\|_2 \leq \delta$

As we showed in the MUSIC algorithm, the residual, $\gamma_{MUSIC}(k) = \frac{\mathbf{d}_{\mathbf{k}}^T \mathbf{P}_{\mathbf{U}_S} \mathbf{d}_{\mathbf{k}}}{\|\mathbf{d}_{\mathbf{k}}\|_2^2}$, will get smaller with better matches. Therefore we formulate the RMUSIC problem with Equation (10).

$$\gamma_{RMUSIC}(k) = \frac{(\mathbf{d}_{\mathbf{k}} - \xi)^T \mathbf{P}_{\mathbf{U}_S}^\perp (\mathbf{d}_{\mathbf{k}} - \xi)}{\|\mathbf{d}_{\mathbf{k}} - \xi\|_2^2} \quad (10)$$

$$s.t. \|\xi\|_2 \leq \epsilon \quad (11)$$

Where $\epsilon > 0$ is a prespecified constant.

Equation (10) forms a quasi-convex, single ratio fractional quadratic program which is optimally solved by Equation (13)

$$\gamma_{RMUSIC}(k) = \min_{\|\xi\|_2 \leq \epsilon} \frac{\|\mathbf{P}_{\mathbf{U}_S}^\perp (\mathbf{d}_{\mathbf{k}} - \xi)\|_2^2}{\|\mathbf{P}_{\mathbf{U}_S}^\perp (\mathbf{d}_{\mathbf{k}} - \xi)\|_2^2 + \|\mathbf{P}_{\mathbf{U}_S} (\mathbf{d}_{\mathbf{k}} - \xi)\|_2^2} \quad (12)$$

$$= \min_{\|\xi\|_2 \leq \epsilon} \frac{\eta_k^2(\xi)}{\eta_k^2(\xi) + 1} \quad (13)$$

$$\text{where } \eta_k(\xi) = \frac{\|\mathbf{P}_{\mathbf{U}_S}^\perp (\mathbf{a}_{\mathbf{k}} - \xi)\|_2}{\|\mathbf{P}_{\mathbf{U}_S} (\mathbf{a}_{\mathbf{k}} - \xi)\|_2}$$

This leaves us with a new optimization problem, determining the optimal η_k , which we denote with η_k^* . We can find η_k^* by optimizing η_k with respect to the ξ , as shown in Equation (14).

$$\eta_k^* = \min_{\|\xi\|_2 \leq \epsilon} \frac{\|\mathbf{P}_{\mathbf{U}_S}^\perp (\mathbf{a}_{\mathbf{k}} - \xi)\|_2}{\|\mathbf{P}_{\mathbf{U}_S} (\mathbf{a}_{\mathbf{k}} - \xi)\|_2} \quad (14)$$

Algorithm 2 RMUSIC

Input: dictionary \mathbf{D} , \mathbf{Y} , ϵ , K

$\mathbf{U}, \mathbf{S}, \mathbf{V} = svd(\mathbf{Y})$

$\mathbf{U}_s = U(1 : K)$

for $k = 1, \dots, K$ **do**

$$\eta_k^* = \min_{0 \leq \theta \leq \epsilon} \frac{\|\mathbf{P}_{\mathbf{U}_S}^\perp \mathbf{d}_{\mathbf{k}}\|_2 - \theta}{\|\mathbf{P}_{\mathbf{U}_S} \mathbf{d}_{\mathbf{k}}\|_2 + \sqrt{\epsilon^2 - \theta^2}}$$

$$\gamma_{RMUSIC}(k) = \frac{(\eta_k^*)^2}{(\eta_k^*)^2 + 1}$$

end for

determine $\hat{\Lambda} = \{\hat{k}_1, \dots, \hat{k}_K\}$ such that $\gamma_{RMUSIC}(\hat{k}_n) < \gamma_{RMUSIC}(j)$ for any $j \notin \hat{\Lambda}$

Output: $\tilde{\mathbf{D}}$

By substitution, we can get a single variable solution for Equation (14), as shown in Equation (15).

$$\eta_k^* = \min_{0 \leq \theta \leq \epsilon} \frac{\|\mathbf{P}_{\mathbf{U}_S}^\perp \mathbf{d}_{\mathbf{k}}\|_2 - \theta}{\|\mathbf{P}_{\mathbf{U}_S} \mathbf{d}_{\mathbf{k}}\|_2 + \sqrt{\epsilon^2 - \theta^2}} \quad (15)$$

This makes the η_k^* problem solvable with a simple grid search over the range $0 \leq \theta \leq \epsilon$. Using Equations (13) and (15), we define the RMUSIC algorithm as seen in Algorithm (2). where $\tilde{\mathbf{D}}$ is the dictionary of the N most important adjusted dictionary entries.

2.3. DANSER

The DANSER algorithm is a CSR method used to determine the relative abundance of a set of spectral signatures for each pixel in the scene. We specify the abundance matrix as \mathbf{C} . The problem is formulated in much the same way as the CSR problem given in Equation (4),

$$\min_{\tilde{\mathbf{D}} \in \mathbb{R}^{M \times K}, \mathbf{C} \in \mathbb{R}^{K \times L}} \frac{1}{2} \|\mathbf{Y} - \tilde{\mathbf{D}}\mathbf{C}\|_{\mathbf{F}}^2 + \lambda \|\mathbf{C}\|_{2,p} \quad (16)$$

$$s.t. \|\mathbf{d}'_{\mathbf{k}} - \mathbf{d}_{\mathbf{k}}\| \leq \epsilon \quad (17)$$

where $\mathbf{C} \geq 0$. Additionally, the variables $0 < p < 1$, and $\epsilon > 0$ are prespecified. The quasi-norm $\|\mathbf{C}\|_{2,p}$ is a row-sparsity promoting norm defined as:

$$\|\mathbf{C}\|_{2,p} = \sum_{i=1}^K \|\mathbf{C}^i\|_2^p \quad (18)$$

where \mathbf{C}^i is the i -th row of \mathbf{C} . While this formulation of the DANSER problem is solvable using alternating optimization, it is far too computationally expensive to be practical. Instead we must modify the problem using a slack variable,

\mathbf{H} , so that we get,

$$\min_{\tilde{\mathbf{D}}, \mathbf{H}, \mathbf{C}} \frac{1}{2} \|\mathbf{Y} - \mathbf{H}\mathbf{C}\|_F^2 + \frac{\mu}{2} \|\mathbf{H} - \tilde{\mathbf{D}}\|_F^2 + \lambda \sum_{i=1}^K (\|\mathbf{C}^i\|_2^2 + \tau)^{p/2} \quad (19)$$

$$s.t. \|\mathbf{d}'_{\mathbf{k}} - \mathbf{d}_{\mathbf{k}}\|_2 \leq \epsilon \quad (20)$$

where $\mu, \tau \geq 0$ and $\mathbf{C} \geq 0$. It can be readily seen that when $\tau = 0$ and $\mu = \infty$, this modified version of the DANSER problem becomes identical to the original problem.

Finally, in order to solve the modified DANSER problem, we must consider the following lemma:

Lemma 2.1 Let $\phi_p(w) = \frac{2-p}{2} (\frac{2}{p}w)^{\frac{p}{p-2}} + \tau w$, where $0 < p < 2$, $\tau > 0$. It can be shown that $\phi_p(w)$ is strictly convex on $w \geq 0$ and satisfies the identity

$$(x^2 - \tau)^{p/2} = \min_{w \geq 0} w \cdot x^2 + \phi_p(w) \quad (21)$$

The solution is uniquely given by

$$w_{opt} = \frac{p}{2} (x^2 + \tau)^{\frac{p-2}{2}} \quad (22)$$

Therefore, the final formulation of the DANSER problem, which can be solved via alternating optimization is given by:

$$\min_{\tilde{\mathbf{D}}\{\mathbf{w}_{\mathbf{k}}\}, \mathbf{H}, \mathbf{C}} \frac{1}{2} \|\mathbf{Y} - \mathbf{H}\mathbf{C}\|_F^2 + \frac{\mu}{2} \|\mathbf{H} - \tilde{\mathbf{D}}\|_F^2 + \lambda \sum_{i=1}^K (\|w_{\mathbf{k}} \mathbf{C}^i\|_2^2 + \phi_p(w_{\mathbf{k}}))$$

While the final forms of the optimizations of $\tilde{\mathbf{D}}\{\mathbf{w}_{\mathbf{k}}\}$, \mathbf{H} , and \mathbf{C} can be seen in Algorithm (3), their derivations are outside the scope of this paper.

3. Experiment

As part of our review of the MUSIC-DANSER algorithm for hyperspectral unmixing, we developed a working recreation of the algorithm using Python 3.7 and tested it on an HSI using a publicly available spectral dictionary. In particular, we were interested in how the algorithm would fair on images that include optically shallow water and specifically whether it could be used to classify seafloor material types for benthic habitat mapping.

Algorithm 3 DANSER

Input: $(\lambda, \tau, p, \mu, \epsilon)$, \mathbf{D}, \mathbf{C} (initialize), \mathbf{Y}

$\tilde{\mathbf{D}} = RMUSIC(\mathbf{D}, \mathbf{Y}, \epsilon, K)$

$w_{\mathbf{k}} = (\frac{p}{2})(\|\mathbf{c}_{\mathbf{k}}\|_2^2 + \tau)^{\frac{p-2}{2}}$

while $\|\mathbf{C}^{(i)} - \mathbf{C}^{(i-1)}\| \leq 10^{-5}$ **do**

Unmixing: $\theta = [\sqrt{w_1 \lambda}, \dots, \sqrt{w_K \lambda}]$

$$\mathbf{H} = (\mu \tilde{\mathbf{D}} + \mathbf{Y}\mathbf{C}^T)(\mathbf{C}\mathbf{C}^T + \mu\mathbf{I})^{-1} \quad (23)$$

$$\tilde{\mathbf{Y}}, \tilde{\mathbf{H}} = \begin{bmatrix} \sqrt{\frac{1}{2}}\mathbf{Y} \\ \mathbf{0} \end{bmatrix}, \begin{bmatrix} \sqrt{\frac{1}{2}}\mathbf{H} \\ Diag(\theta) \end{bmatrix} \quad (24)$$

$$\mathbf{F}, \mathbf{G} = \tilde{\mathbf{Y}}^T \tilde{\mathbf{H}}, \tilde{\mathbf{H}}^T \tilde{\mathbf{H}} \quad (25)$$

for $k = 1, \dots, K$ **do**

$$\mathbf{c}^k = \left(\frac{\mathbf{F}_{:,k} - \mathbf{C}^T \mathbf{G}_{:,k} + (\mathbf{c}^k)^T \mathbf{G}_{\mathbf{k},\mathbf{k}}}{\mathbf{G}_{\mathbf{k},\mathbf{k}}} \right)_+ \quad (26)$$

end for

$$\mathbf{H} = (\mu \tilde{\mathbf{D}} + \mathbf{Y}\mathbf{C}^T)(\mathbf{C}\mathbf{C}^T + \mu\mathbf{I})^{-1} \quad (27)$$

for $k = 1, \dots, K$ **do**

$$\mathbf{d}_{\mathbf{k}}' = \begin{cases} \mathbf{h}_{\mathbf{k}}, & \text{if } \|\mathbf{h}_{\mathbf{k}} - \mathbf{d}_{\mathbf{k}}\|_2 \leq \epsilon \\ \mathbf{d}_{\mathbf{k}} + \epsilon \frac{\mathbf{h}_{\mathbf{k}} - \mathbf{d}_{\mathbf{k}}}{\|\mathbf{h}_{\mathbf{k}} - \mathbf{d}_{\mathbf{k}}\|_2}, & \text{otherwise} \end{cases} \quad (28)$$

end for

$$w_{\mathbf{k}} = (\frac{p}{2})(\|\mathbf{c}_{\mathbf{k}}\|_2^2 + \tau)^{\frac{p-2}{2}} \quad (29)$$

end while

Output: \mathbf{C}

3.1. AVIRIS

NASA's AVIRIS mission is a high altitude, airborne hyperspectral imager. It operates at 224 contiguous bands in the visible and infrared portion of spectrum between 380 and 2500 nm. Each band corresponds to an approximately 10 nm interval. AVIRIS has a swath width of 11 km and spatial resolution of 20 m.

As noted above, our main interest in this project was to explore the use of MUSIC-DANSER for benthic habitat mapping. With this in mind, we selected a site off the West coast of the Island of Hawai'i, at the Puu Alii Bay. Figure 1 shows a Google Maps satellite image of the extent of the study site.



Figure 1. Puu Alii Bay study site off the West coast of the Island of Hawai'i.

Figure 2 shows the same spatial extent but from the band 30 of the AVIRIS HSI.

3.2. USGS Spectral Dictionary

The USGS spectral dictionary is a library of the spectral signature of thousands of materials collected by the United States Geological Society via field, laboratory, and airborne methods. The span of the electromagnetic spectrum covered by the spectra of the various materials differs based on the method used to collect the data, with some entries covering the spectrum all the way from ultraviolet to far infrared. Due to this fact, we chose to use only the entries in the library collected by previous AVIRIS missions in order to meet the time constraints of this project. This left me with a total 2457 spectral signatures to use for classification of the AVIRIS HSI. Figure 3 shows a colored matrix of the spectral dictionary with the vertical axis indicating the band number, the horizontal axis indicating the dictionary entry number,

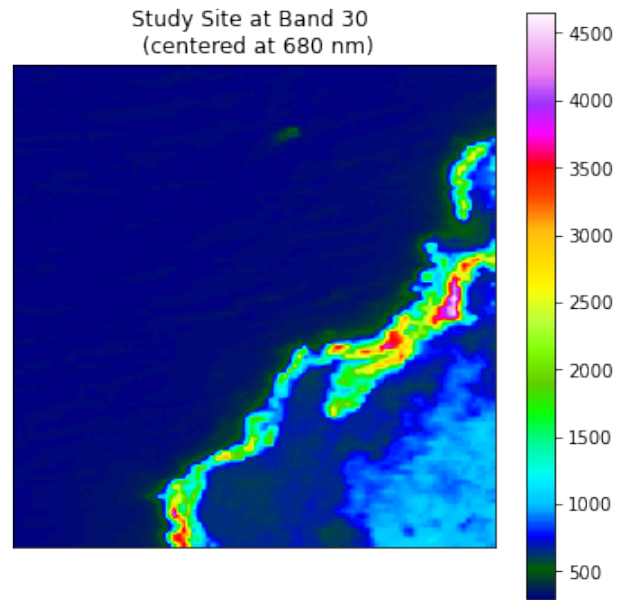


Figure 2. AVIRIS image of Puu Alii Bay at band 30 (centered at 680 nm).

and color representing intensity. Darker blue represents lower intensity while greens and reds indicate increasingly greater intensity.

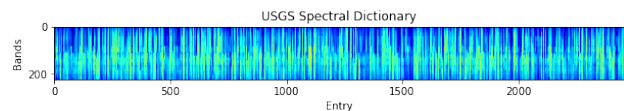


Figure 3. USGS Spectral Library with only AVIRIS collected samples.

3.3. Preprocessing

Before applying the algorithms to the Puu Alii Bay HSI and the USGS spectral dictionary, we first performed a brief preprocessing of the data in order to reduce noise. It is well documented that certain AVIRIS bands are particularly sensitive to noise, and so we removed those bands from the calculations. We selected the bands to remove by calculating the SNR and removing any bands with an SNR below -3.5 db. Figure 4 shows a plot of the SNR and it can clearly be seen where bands were removed.

4. Results

After acquiring and preprocessing the data, we applied the MUSIC-DANSER algorithm. The first step in this process

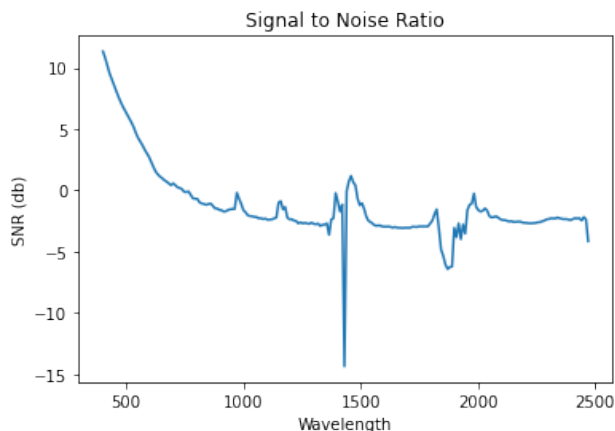


Figure 4. Signal to Noise Ratio evaluation of the AVIRIS bands.

was to apply the RMUSIC algorithm using the preprocessed HSI as \mathbf{Y} and the USGS spectral dictionary as \mathbf{D} . Since this project is a review and not a rigorous analysis, we set K arbitrarily to 20 as that it provided a large enough set of results to analyze without eating up too much computation time. Figure 5 shows the residuals of the RMUSIC algorithm. An alternative method for determining K is HySiMe algorithm, which we intend to investigate further in the future but is outside the scope of this project. It can be readily seen that, as expected, the bulk of the dictionary entries cluster at larger residuals, with only a handful at the lowest tier of residuals. Table 1 shows the residual values of the 20 materials detected by RMUSIC with their associated dictionary entry names.

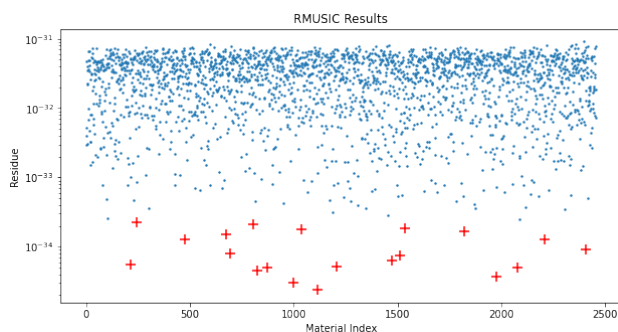


Figure 5. Residuals of the dictionary entries from the RMUSIC algorithm

Next we applied the DANSER algorithm using the AVIRIS HSI as \mathbf{Y} , and the results of RMUSIC as $\tilde{\mathbf{D}}$. The parameters λ , τ , p , μ , and ϵ were set to 0.5, 10^{-6} , 0.5, 10^5 , and $\frac{1-0.85}{1+0.85} \min(\|\mathbf{d}_k\|_2)$, respectively. These were the suggested parameter values from Fu et al., 2016. The resulting abun-

Table 1. RMUSIC residual values by material from most important (top) to least important (bottom).

MATERIAL	RESIDUAL ($\times 10^{-35}$)
PLASTIC LDPE GDS405 BLACK	2.36
BONE BLACK GDS808	2.99
CARBON BLACK GDS68 SM.AP.	3.68
OIL92 WATER08 DWH10-3 0.05MM	4.56
NICKEL POWDER SA-577995 NANO	5.00
IRON OXIDE GDS810 (MARS) BLK	5.07
CARBON BLACK GDS68	5.21
MARSHWATER CRMS121v69-NOGLNT	5.52
PLASTIC ABS GDS341 BLACKPIPE	6.35
SEAWATER COAST CHL SW1	7.58
MARSH WATER CRMS322v84A SUNL	7.89
SEAWATER OPEN OCEAN SW2 LWCH	9.15
ILMENITE HS231.3B NIC4BCU RREF	12.61
ASPHALT TAR GDS346 BLCK ROOF	12.88
WATER+MONTMOR SWY-2+0.50G-L	14.96
OIL92 WATER08 DWH10-3 0.1 MM	16.80
MAGNETITE HS78.1B ASDFRB	17.94
GALENA HS37.3FG ASDFRB	18.46
ALLANITE HS293.4B ASDFRB	21.13
PLASTIC PIPE GDS342 BLACK	22.75

dance maps are shown in Figure 6.

5. Discussion

5.1. RMUSIC

It is clear from Figure 5 that the RMUSIC algorithm was effective in ranking the spectra in the dictionary based on their importance to the scene. We clearly see that the majority of the spectra are cluster at the larger residual values between 10^{-32} and 10^{-31} . Additionally, we find fewer and fewer dictionary entries as the residuals get smaller. While this analysis is encouraging, it should be noted that a similar figure shown in Fu et al., 2016 displayed a range of residuals from 10^0 to 10_{-5} . While this difference does not necessarily indicate an error in the implementation of the algorithm in the case of this project, it does raise concerns about the lack of preprocessing done on the HSI before implementing the algorithms. It is possible that a mismatch in units between the dictionary entry intensities and the HSI intensity resulted in a significant shift in the scale of the RMUSIC residuals. The reason we did not explore preprocessing of the HSI more thoroughly was due to the time constraints of this project. In future applications of these algorithms or others, we will need to better explore the metadata and understand why scale shifts of this magnitude occur.

Additionally, we cannot discuss the results of the RMUSIC algorithm without addressing the obvious fact that the materials extracted from the dictionary to represent the HSI are, in several cases, blatantly incorrect. In particular, the pres-

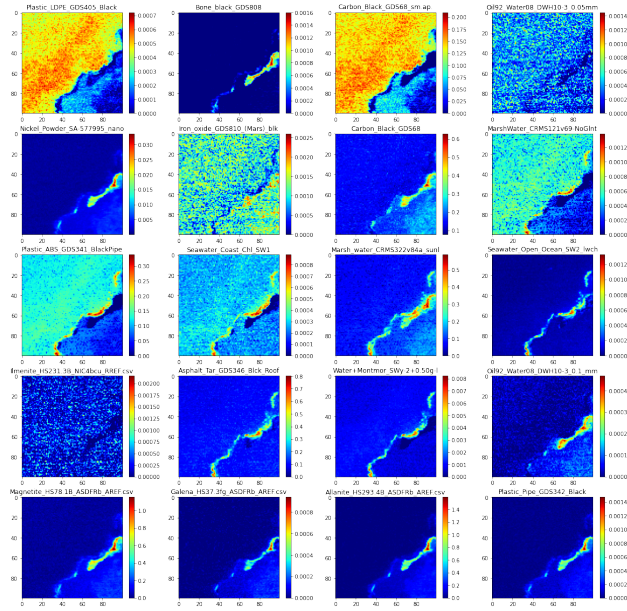


Figure 6. DANSER Abundance Maps from the RMUSIC selected endmembers.

ence of man-made materials such as Low Density Polyethylene (LDPE), Plastic Pipe, and Plastic Acrylonitrile Butadiene Styrene (ABS) are egregious misclassifications. While troubling, there are explanations for the presence of these materials in the scene. First of all, errors in the implementation of the RMUSIC algorithm cannot be ruled out at this point. However, assuming the algorithm was implemented correctly, it is also possible the the HSI used in this experiment was a TOA (top of atmosphere) image, as opposed to surface reflectance, and therefore corrupted by atmospheric effects. There are many methods to correct for atmospheric effects in HSI, but it was not clear whether these corrections were made ahead of time by NASA’s AVIRIS data managers. Future exploration of this concern is warranted. Other head scratching results, such as Black Carbon, Bone Black, and Asphalt Tar, are more easily explainable as the result of a close spectral match with what appears to be ultramafic lava flows directly off the coast.

5.2. DANSER

Figure 6 shows that the DANSER algorithm was particularly effective in differentiating the spectra of the open ocean, the optically shallow coastal regions, and the land. Although there are some exceptions, and the materials used to classify these landcover types are blantly incorrect, we consider this result to be highly encouraging for benthic habitat mapping. The abundance maps clearly show that the algorithm is able to precisely separate the optically shallow regions

from the deeper ocean, as well as capture the complexity of these optically shallow regions.

It should be noted that a few of the resulting abundance maps, such as Ilmenite, Mars Iron Oxide, and Oil/Water 92/8 at 0.05mm, are highly noisy. The high levels of noise in these abundance maps could be due to atmospheric effects, which further supports the hypothesis that this is a TOA HSI. Again, further exploration of this hypothesis is warranted.

6. Conclusion

The purpose of this project was to review the MUSIC-DANSER hyperspectral unmixing algorithm presented in Fu et al., 2016 and explore its use for benthic habitat mapping. We implemented an experiment using an AVIRIS scene from the Puu Alii Bay off the West coast of the Island of Hawai’i and the USGS spectral dictionary AVIRIS data. The algorithm produced a list of the 20 most important materials in the scene as well as relative abundance maps for each of these materials. Our results show that the RMUSIC algorithm was able to rank the dictionary entries based on their importance to the scene, however there are still questions about the specific entries that the algorithm deemed most important. The DANSER algorithm was able to produce abundance maps for each of these materials using collaborative sparse regression. These maps show some clear misclassifications that are possibly the result of applying the algorithms to TOA data, as opposed to an atmospherically corrected surface reflectance image. Despite these results, we still believe the MUSIC-DANSER algorithm holds great promise in the field of benthic habitat mapping. In future work we hope to double check our implementation of the algorithms for errors, further explore the AVIRIS and USGS metadata for potential sources of error, and eventually produce a benthic habitat map from HSI data. This product could be fused with our current research on bathymetric modelling using NASA’s ICESat-2 lidar satellite to generate 3D models of the seafloor. We hope this future work will become a keystone of our doctoral dissertation and a strong contribution to the field of earth observation and remote sensing.

References

- [1] X. Fu, W. Ma, J. M. Bioucas-Dias and T. Chan. *Semib-lind Hyperspectral Unmixing in the Presence of Spectral Library Mismatches*. IEEE Transactions on Geoscience and Remote Sensing, vol. 54, no. 9, pp. 5171-5184, Sept. 2016.